

Chandra Observations of Embedded Young Stellar Objects

Katsuji Koyama

*Department of Physics, Graduate School of Science, Kyoto University,
Kita-Shirakawa, Sakyo-ku, Kyoto, 606-8502, Japan*

Abstract. This paper reviews the results of the *Chandra* deep exposure observations on star forming regions. The ρ Ophiuchi (ρ Oph) cloud cores B-F reveal ~ 100 X-ray sources above the detection limit of $\sim 10^{28}$ ergs s^{-1} . About 2/3 of the X-ray sources are identified with an optical and/or infrared (IR) object, including significant numbers of class I sources. The class I sources exhibit higher temperature plasma than those of class II and III sources. These features are confirmed with a larger number of X-ray sources in the Orion molecular clouds 2 and 3 (OMC 2 and 3).

Hard X-ray emissions are found from the sub $mm - mm$ dust cores, MMS 2 and MMS 3 in the northern part of OMC 3. These cores show outflows in the radio and IR bands, hence are in a very early phase of star formation, possibly in the class 0 phase. The spectra are heavily absorbed suggesting that the X-ray sources are embedded in the cores.

The giant molecular cloud Sagittarius B2 (Sgr B2) exhibits more than dozen X-ray sources, two of which are associated with the HII complex Sgr B2 Main (the ultra compact HII regions F-I). These show an absorption of $\gg 10^{23}$ Hcm^{-2} , which is the largest among the known stellar X-ray sources. The X-ray source in the HII regions F-I shows strong K-shell transition lines from He-like and neutral irons, while that in the east of the HII region I has only a weak line. No strong X-ray emission is found from any other HII complexes; hints of weak X-rays are found from only Sgr B2 North (the HII region K) and South (H).

The Monoceros R2 cloud exhibits X-ray emissions from young high-mass stars. IRS 1, possibly in zero-aged main-sequence, shows rapid time variability and a thin thermal spectrum of ~ 2 keV temperature. Similar X-ray behaviors are found from younger high-mass stars, IRS 2 and IRS 3. These X-ray features are in contrast to the low temperature plasma (≤ 1 keV) and moderate variability found in high-mass main-sequence stars.

X-rays from 7 brown dwarfs and candidates are found in the ρ Oph cloud cores A-F, which comprise 40% of those selected with the IR observations. The X-rays are variable with occasional flares. The X-ray spectra are fitted with a thin thermal plasma of 1-3 keV, with the luminosity ratio of X-ray to bolometric of $10^{-3} - 10^{-5}$. These properties are essentially the same as those of low-mass pre-main sequence and dMe stars.

1. Introduction

Young stellar objects (YSOs) evolve from molecular cloud cores through protostars and pre main-sequence (PMSSs) to zero-aged main-sequence stars (ZAMSSs). The evolutionary track of low mass YSOs can be well traced with the infrared (IR)-*mm* band spectra. Class 0 stars (class 0s), the early phase of protostars, show the spectral peak at the *mm* band, arising from the gas envelope. Class I stars (class Is), the later phase of protostars, exhibit the emission peak at the mid- to far-IR wavelengths, and the spectra are still dominated by the accreting gas envelope. T Tauri stars (TTSs) are the quasi-static mass-condensation phase after the dynamical mass accretion phase of protostars, and are divided into class IIs and IIIs; the formers correspond to classical T Tauri stars (CTTSs), which have a gas disk and show the near- to mid-IR excess emission from the disk. When the accretion disk disappears, CTTSs evolve to weak-lined T Tauri stars (WTTSs) or class IIIs, which have a black body spectrum from the stellar photosphere with the peak at near-IR. This phase lasts until hydrogen burning is ignited, which is the phase of ZAMSSs.

TTSs (class IIs and IIIs) have been known to exhibit fairly strong X-rays with occasional flares. The X-ray spectra are described with a thin thermal plasma model of a temperature ranging from 1 to a few keV. The X-rays are similar to, but have a larger flux and a higher temperature than those of the sun, which leads to the general consensus that the X-ray origin is due to the enhanced solar-type magnetic activity. The X-rays become less active as the low mass stars evolve to main sequence stars (MSSs) (for reviews, see Feigelson & Montmerle 1999).

X-rays from class I protostars are discovered with either the hard X-ray imaging instrument on board *ASCA* (Koyama et al. 1996, Kamata et al. 1997) or the deep exposure observations with *ROSAT* (e.g. Grosso et al. 2000). The X-ray features are similar to those of more evolved stars, like TTSs, hence would be also due to the solar-type magnetic activity. However, more quantitative study on protostellar X-rays in comparison with TTSs has not been done, due to very limited samples of protostars; the X-ray detection rate from class Is was only 10%, no X-ray sample from class 0 protostars, the youngest phase of the stellar evolution, has been found.

Since the evolution of high mass YSOs is very rapid, the evolutionary classifications (or phase) are not clear-cut. Also the X-ray study on high mass YSOs is far behind those of low mass stars, because of limited samples. The *ASCA* satellite has found hard X-rays from the center of giant molecular clouds (GMCs), the site of high-mass star formation (e.g. Yamauchi et al. 1997; Hofner & Churchwell 1997; Sekimoto et al. 2000; Hamaguchi, Tsuboi, & Koyama 2000). However, the limited spatial resolution of $\sim 1'$, did not allow us to uniquely resolve high mass YSOs in the GMCs, due to their relatively large distance and high density of stellar populations.

Stellar X-rays have appeared well before the Hydrogen burning phase (MSSs), regardless of the stellar mass. Therefore it may be conceivable that brown dwarfs, the sub-stellar object with the mass below the hydrogen burning limit of $0.08M_{\odot}$, also emit X-rays. In fact, *ROSAT* discovered X-ray emission from brown dwarfs (Neuhäuser & Comerón 1998). However the number of, and the spectrum/timing information of, the X-ray detected brown dwarfs are still poor.

As mentioned above, most of the previous X-ray studies on YSOs have been concentrated on the low mass stars in a TTS phase (class IIs and IIIs). This paper extends the X-ray frontier toward three directions, using the hard X-ray instruments with a fine spatial resolution of *Chandra*: the X-ray emission from high mass YSOs, protostars (class 0s and Is), and young blown dwarfs (BDs). The study is based on the recent *Chandra* results. The star forming regions referred in this paper are: ρ Ophiuchi (ρ Oph), Orion Molecular Clouds 2 and 3 (OMC 2 and OMC 3), Sagittarius B2 (Sgr B2) and Monoceros R2 (Mon R2). Detailed and individual reports are: Imanishi, Koyama & Tsuboi (2001); Tsuboi et al. (2001); Tsujimoto et al. (2001a, b); Takagi, Murakami & Koyama (2001); Kohno, Koyama & Hamaguchi (2001); and Imanishi, Tsujimoto & Koyama (2001).

2. Low Mass Protostars

In the *Chandra* ACIS-I observation on the ρ Oph cores B-F, we detect ~ 100 X-ray sources above the threshold of $\sim 10^{28}$ ergs s $^{-1}$, of which 18 are identified with class Is¹. In the same field, we find 26 class Is in the IR-band star catalogs. Thus about 70% of the IR-selected class Is are X-ray sources, which is higher ratio than that with *ROSAT* PSPS of about $\sim 10\%$ (Carkner, Kozak, & Feigelson 1998). The high detection rate of class Is ($\sim 70\%$) with *Chandra* is primary due to the high sensitivity, especially in the hard X-ray band.

Having reasonable numbers of X-ray samples of low mass YSOs (class I - III), we fit the X-ray spectra with a thin thermal plasma model for all the bright X-ray sources, then find that the X-ray temperatures and absorptions of class Is are generally larger than those of class IIs and IIIs. Also X-ray flares from class Is show a hint of higher duty ratio, temperature and luminosity, than those from more evolved class II and III stars.

A remarkable finding is a giant flare from YLW 16A with the peak luminosity of $\sim 10^{31}$ ergs s $^{-1}$. At the flare, the temperature rises to ~ 10 keV with the 6.7 keV line emission from He-like irons. We also find the 6.4 keV line of equivalent width ~ 100 eV, which would be fluorescence from cold irons in the circumstellar gas. Since no time-lag is found between the 6.4 keV line and continuum flux, the site of fluorescence should be very near the protostar, possibly the accretion disk. The large equivalent width favors a disk face-on geometry. Likewise, the 6.4 keV line is a powerful diagnostics for the structure of the gas envelope of YSOs.

A larger number of X-ray emitting low-mass YSOs is obtained from OMC 2 and 3. *Chandra* detects ~ 400 X-ray sources in a $17' \times 17'$ field of the clouds. Our unified spectral analyses for all the X-ray bright sources (~ 120) reveal similar X-ray features as those found in the ρ Oph molecular cloud; X-ray temperatures

¹Class I sources are defined by the near- to mid-IR band or near- to far-IR band spectra (André & Montmerle 1994; Casanova et al. 1995; Chen et al. 1995; Chen et al. 1997; Motte, André, & Neri 1998; Luhman & Rieke 1999; Grosso et al. 2000). Since the classifications in these papers are not fully consistent with each other, I simply regard a class I if any of the papers referred to be a class I source

and absorptions of class Is are generally larger than those of class IIs and IIIs (Tsujiimoto et al. 2001a).

Table 1. X-rays from Class 0 Candidates

Position ¹	N_{H} ²	L_{x} ³	Associated sources ⁴
18".22, -34".0	25(12-54)	2	MMS 2, CSO 6, H ₂ flow B, HH 331, VLA 1, H ₂ Jet
18".93, -51".0	14(7-34)	1	MMS 3, CSO 7, H ₂ flow D

Temperature and abundance are fixed to be 3.2 keV and 0.3 solar, respectively. Parentheses indicate 90% confidence range.

(1) Off set = $(05^{\text{h}}35^{\text{m}}, -05^{\circ}00')$ _{J2000}

(2) Absorption in units of 10^{22} Hcm⁻²

(3) The 0.5-10 keV band luminosity in units of 10^{30} ergs s⁻¹

(4) Yu, Bally, & Devine (1997); Reipurth (1999); Yu et al. (2000);

Reipurth, Rodríguez & Chini (1999); Tsujimoto et al. (2001b)

A notable result is the discovery of highly absorbed X-ray sources from the dust condensations MMS 2 (CSO 6) and MMS 3 (CSO 7) in the north of OMC 3 (Tsuboi et al. 2001). Since the photon statistics is limited, the spectra are fitted with a thin thermal model by fixing the temperature to be 3.2 keV, following the results of other sources in this region. Table 1 shows the results of the two X-ray sources. The absorption columns are $(1-3) \times 10^{23}$ Hcm⁻², which are larger than those of class Is obtained with *ASCA* (Kamata et al. 1997; Tsuboi et al. 2001) and *Chandra* (Imanishi, Koyama & Tsuboi 2001). Consequently, these X-ray sources are really embedded in the cloud cores.

MMS 2 is associated with a prominent H₂ flow B (Yu, Bally, & Devine 1997), a Herbig-Haro object HH 331 (Reipurth 1999) and a 3.6-cm-radio source VLA 1 which is most likely due to a thermal jet (Reipurth, Rodríguez & Chini 1999). MMS 3 seems to be associated with a shock-excited H₂ flow D (Yu, Bally, & Devine 1997). In addition, Yu et al. (2000) and Aso et al. (2000) found molecular outflows of ¹²CO $J = 2-1$ and HCO⁺ from the MMS 2-3 region. These facts support that MMS 2 and 3 probably contain class 0 sources. In more detail, we resolve the X-ray emission at MMS 2 into three sources; two are associated with K -band sources discovered with our follow-up deep IR observations (Tsujiimoto et al. 2001). The other X-ray source has no IR-counterpart, instead an IR-jet is found. The hard X-ray source at MMS 3 shows no K -band counterpart even with our deep IR observations. Thus these two X-ray sources would be class 0s in the cloud cores MMS 2 and 3 (Tsujiimoto et al. 2001b).

3. High Mass Young Stars

The giant molecular cloud Sgr B2, located at a projected distance of only 100 pc from the Galactic center (GC), is one of the richest star forming regions (SFR)

in our Galaxy. Due to its proximity to the GC, Sgr B2 is heavily obscured in the optical, even near infrared (NIR) and soft X-ray bands. Accordingly, the star formation activity has been traced mainly with the radio and far infrared (FIR) bands. The radio continuum bands have revealed nearly 60 ultra compact (UC) HII regions lying along the north-to-south elongation, which are also traced by molecular lines and FIR (Gaume et al. 1995; De Pree, Goss & Gaume 1998). Bipolar outflows are found from two of the HII complexes, Sgr B2 Main and North (Lis, et al. 1993). Also clusters of OH, H₂O and H₂CO masers are found near the HII regions (Mehringer, Goss & Palmer 1994). Thus Sgr B2 is comprised of many clusters of high mass YSOs.

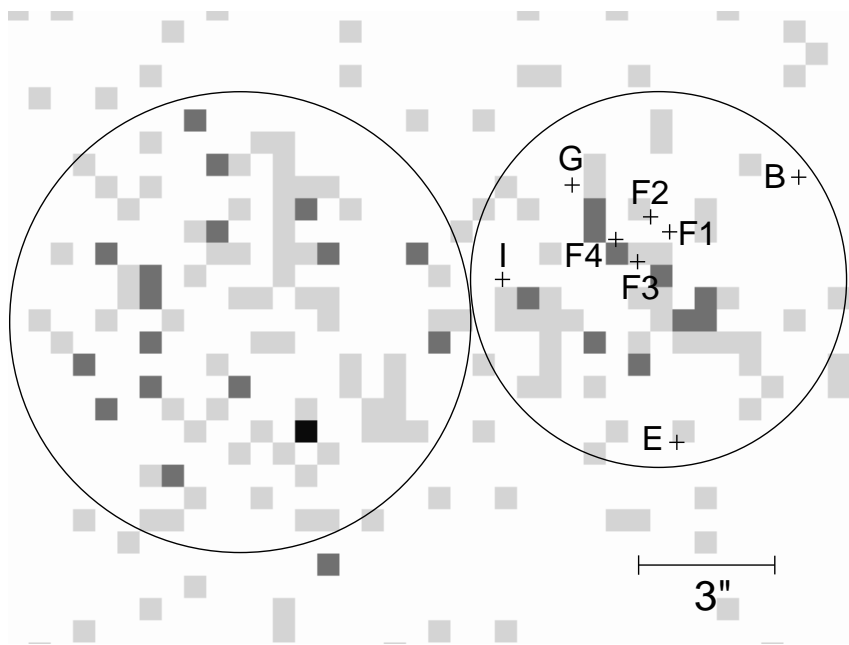


Figure 1. The X-ray image near the HII complex Sgr B2 M. Crosses are the position of ultra compact HII regions (Gaume et al. 1995). The X-ray spectra are obtained from the circles (see text).

More than a dozen X-ray sources are found from the Sgr B2 cloud region (Takagi, Murakami & Koyama 2001), of which the second and third brightest (here, sources A and B) are located in the HII complex Sgr B2 M (Main). Figure 1 shows the X-ray image in the 2-10 keV band, overlaid on the positions of UC HII regions. Source A seems to be extended lying in the UC HII regions F and I, hence would be comprised of several point sources. The X-ray peak comes near the position of the brightest UC HII, F3d (De Pree, Gross and Gaume 1998), which is also considered to be an engine of the HC₃N bipolar flow (Lis et al. 1993). From the HII and outflow data, this X-ray peak may correspond to a very high mass (e.g. O6, assuming ZAMS) young (well below 10⁵ year) star.

Table 2. X-ray sources in the Sgr B2 Main Complex

Source ¹	kT^2	N_{H}^3	L_x^4	EW^5
A	10 (4.1-30)	4.0 (1.9-8.8)	8	0.6
B	4.8 (≥ 1.1)	4.0 (2.4-7.3)	13	-

Parentheses indicate 90% confidence range.

(1) A: HII regions F-I, B: The east of HII region I (Gaume et al. 1995)

(2) Temperature in units of keV

(3) Absorption in units of 10^{23} Hcm⁻²

(4) Luminosity in the 2-10 keV band in units of 10^{32} erg s⁻¹

(5) Equivalent width of the 6.4 keV line in units of keV

The X-ray components of source A are lying along the UC HII regions F3, F4 and G. Figure 2 (right) shows the composite spectrum of source A, taken from the circle given in figure 1 (right). The spectrum is nicely fitted with a thin thermal model as is shown in table 2 and figure 2 (right).

Source B is also a complex lying in the east of the HII region I, as is seen in the left circle of figure 1. No association with HII region may indicate that source B is a cluster of high mass PMSSs. Figure 2 (left) and table 2 show the X-ray spectrum and the best-fit thin thermal model. Like source A, the best-fit temperature and absorption are the largest among the known stellar X-ray sources. This supports the hypothesis that sources A and B are lying at and near the center of the Sgr B2 cloud, and demonstrate that hard X-rays are very powerful to discover deeply embedded stars even if they are suffered with a large optical extinction of $A_v \sim 200-300$ mag.

The absorption corrected luminosity in the 2-10 keV band for sources A and B are 8×10^{32} ergs s⁻¹ and 13×10^{32} ergs s⁻¹, respectively. Suppose these X-ray sources are complex of several high mass YSOs, then the individual luminosity would be in the order of 10^{32} ergs s⁻¹, similar to the nearest high mass YSO, θ C Ori of spectral type O6-7 (Schulz et al. 2000), and larger than those of younger stars, IRS 1-3 in Mon R2 (Kohno, Koyama & Hamaguchi 2001). The high temperature plasma like 5-10 keV is also found from these high mass YSOs. Other than the HII regions F-I, no clear X-rays are found from most of the UC HII regions; we see only a hint of weak X-rays from the HII regions K (Sgr B2 North) and H (Sgr B2 South).

A notable feature of source A is strong lines at 6.7 keV and 6.4 keV. The former is the K-shell transition line from He-like irons in a thin hot plasma. The iron abundance is more than 5 times of solar, which is significantly larger than that from any other high-mass SFRs (Kohno Koyama & Hamaguchi 2001; Schulz et al. 2001; Yamauchi et al.1997). The later line (6.4 keV line) may be due to neutral or low-ionization irons in the dense circum/inter stellar medium irradiated by the central stars. We note that even stronger 6.4 keV line is found from a larger region extending over the whole Sgr B2 cloud, which may

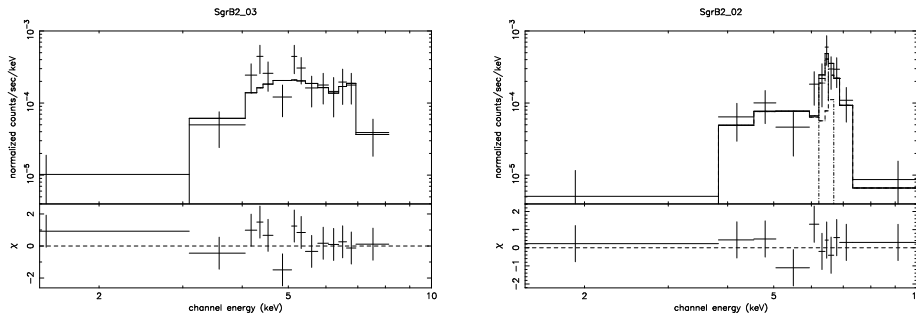


Figure 2. Right: The X-ray spectrum and the best-fit model (solid histogram) of a thin thermal plasma with a 6.4 keV line (the dotted histogram) for source A. Left: Same as the right figure but for source B.

be originated from a very luminous external X-ray source (Murakami, Koyama & Maeda 2001). The iron abundance of source B, in contrast to source A, is sub-solar. Are the chemical abundances really different or is the X-ray emission mechanism different with each other, or is there any other reason ? In any case, how does nature make such a large difference between these two star clusters separated only 0.2-0.3 pc in projection ?

We have observed another high-mass SFR, the Mon R2 cloud located at a distance of 830 pc (Racine 1958) toward the anti-GC direction. Figure 3 shows the ACIS-I image of the central region of the cloud. We see heavily absorbed X-rays from high mass YSOs, IRS 1SW, IRS 2, IRS 3NE and a_5 ². The X-ray features with the best-fit thin thermal model are listed in table 3.

IRS 1 is located in a compact HII region in an IR shell (Massi, Felli, & Simon 1985). It has been resolved into two IR stars, IRS 1SW and NE (Howard, Pipher & Forrest 1994). IRS 1SW is exciting the compact HII region with a predicted luminosity of $\geq 10^4 L_\odot$, hence would be a B0 of zero-aged main sequence (ZAMS). The IR source a_5 has been less studied, hence is not well known. It is associated with a small IR nebulosity and has a similar IR spectrum and bolometric luminosity to those of IRS 1SW, hence may be a similar mass star, early B or late O type. Since a_5 has no HII region, it may be younger than IRS 1SW. We find that IRS1 SW and a_5 are strong and heavily absorbed X-ray sources, consistent with their $H - K$ values. These show a high temperature plasma of $\sim 2-3$ keV and a rapid time variability including flare-like events, in contrast to high mass MSSs with lower temperature plasma of ≤ 1 keV and relatively stable light curve. We thus suspect that IRS 1SW and a_5 have higher magnetic activity than that of stellar wind. The X-ray luminosity is $\sim 10^{31}$ erg s^{-1} , which is significantly higher than that of low mass YSOs.

²For the IR sources, we refer the original naming by Beckwith et al. (1976)

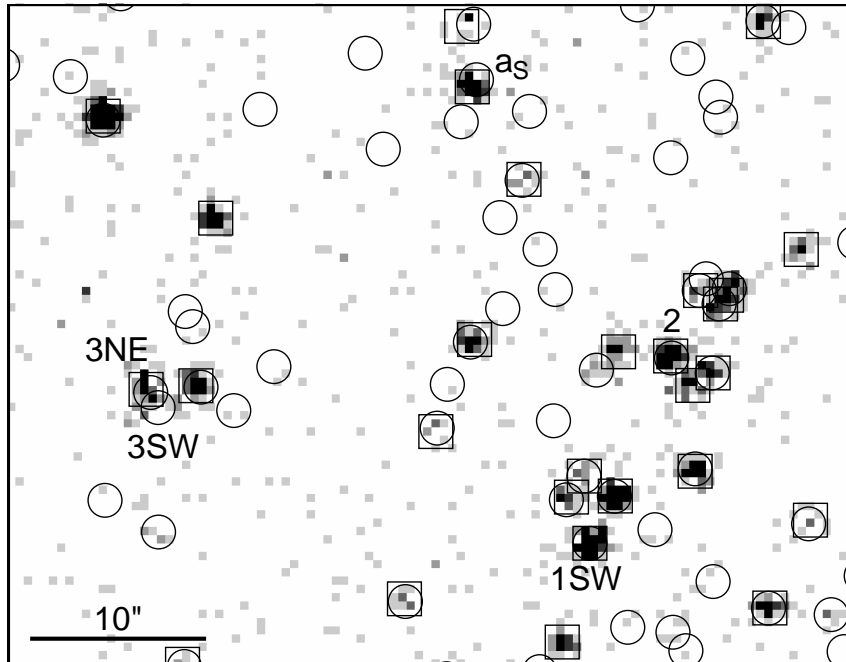


Figure 3. Expanded view of the Mon R2 cloud core of a $50'' \times 50''$ region. Circles and squares indicate the positions of infrared and X-ray sources, respectively (Carpenter et al. 1997; Kohno, Koyama & Hamaguchi 2001). High mass YSOs are shown with the labels of a_s , (IRS) 1SW, (IRS) 2, (IRS) 3NE and 3SW.

IRS 2 is an illuminating source of the IR shell. The bolometric luminosity is $\sim 0.5 \times 10^4 L_\odot$, hence would be a high mass YSO of $8-10 M_\odot$ (Howard, Pipher & Forrest 1994). The infrared spectrum of IRS 2 (also IRS 3) shows deep absorption features in the water-ice and silicate bands, which is a signature of a cluster of several young embedded sources (Smith, Sellgren & Tokunaga 1989; Sellgren, Smith & Brooke 1994; Sellgren et al. 1995). Thus IRS 2 may contain high mass star(s) in younger phase than IRS 1 at ZAMS. Our *Chandra* observation reveals that IRS 2 has the highest plasma temperature (~ 10 keV) and the largest absorption column density ($\sim 10^{23} \text{ Hcm}^{-1}$) among the bright sources in the Mon R2 cloud. Large absorptions have been reported from embedded low mass stars, like class I or 0 protostars (Koyama et al. 1996; Imanishi, Koyama & Tsuboi 2001). Therefore, the heavily absorbed hard X-ray source at IRS 2 is very likely to be a high mass YSO. Since the X-ray time variation is long enough to be rotational modulation, it may be arisen from the interaction of stellar wind with magnetosphere (e.g. Gagne et al, 1997). However, IRS 2 has neither HII region, hence no strong UV field, nor strong stellar wind. Furthermore *ASCA* detected a big flare from the position of IRS 2, although possible source confusion can

not be excluded (Hamaguchi, Tsuboi & Koyama 2000). Therefore, X-rays from IRS 2 are likely magnetic origin.

IRS 3, the brightest source in the near- and mid-IR bands in Mon R2, is another active star forming site. The presence of H₂O and OH masers and a well-developed molecular outflow indicate that IRS 3 is still in a phase of dynamical mass accretion. From the velocity and size of the outflow, the age is estimated

Table 3. High mass YSOs in Mon R2

Name	kT^1	N_{H}^2	L_{x}^3
IRS 1SW	1.9(1.3-2.8)	4.7(3.5-6.4)	1 (0.6-2.0)
as	2.6(1.6-6.2)	6.0(4.0-9.2)	0.6(0.4-1.6)
IRS 2	10.9(\geq 2.0)	9.1(5.7-17)	0.6(0.5-2.0)

Parentheses indicate 90% confidence range.

(1) Thin thermal temperature in units of keV

(2) Absorption in units of 10^{22} Hcm⁻²

(3) The 0.5-10 keV band luminosity in units of 10^{31} ergs s⁻¹

to be $\sim 10^5$ years, hence would contain a youngest high-mass star in the cloud. IRS 3 has been resolved into two sources IRS 3NE and 3SW, of which the former (IRS 3NE) exhibits heavily absorbed hard X-rays, hence is a candidate of a high mass YSO embedded in the cloud core. The infrared polarimetry reveals that the interstellar magnetic field is compressed from the neighbor of the GMCs (e.g., Yao et al. 1997). If the magnetic field is connecting the stellar surface and the accreting gas disk, it can be twisted, amplified and reconnected by the differential rotation. Then a high temperature plasma is produced by the release of the magnetic energy (Tsuboi et al. 2000; Montmerle, et al. 2000). The outflow found from IRS 3 is also explained by this scenario (Hayashi, Shibata & Matsumoto 1996).

Since the majority of stars in the universe seem to form in binary pairs, one may argue that these high mass stars are binaries with a low mass companion, and the low mass YSO may be responsible for the X-ray emission. The X-ray luminosity of these high mass YSOs, $\sim 10^{30-31}$ ergs s⁻¹, is however significantly larger than that of typical low mass YSOs of $\sim 10^{28-29}$ ergs s⁻¹. Thus contribution of low mass companion, if any, may be a small fraction of the bulk X-rays observed from the high mass YSOs.

Here we propose a working hypothesis for the study of X-ray evolution of high mass YSOs; high mass stars produce variable and hard (2-10 keV) X-rays due to the magnetic activity in PMS (source B in Sgr B2, IRS 2 and IRS 3NE in Mon R2). It continues until ZAMS (source A in Sgr B2, IRS 1SW in Mon R2), then gradually decline to stellar wind dominant activity. Finally, in the main sequence phase, high mass stars predominantly emit soft (≤ 1 keV temperature) X-rays originated from the strong stellar wind (e.g. the Orion Trapezium stars).

4. Young Brown Dwarfs

Chandra made two deep exposure observations on the center region of the ρ Oph cloud core A and cores B-F. We search for X-ray emission from the brown dwarf catalogs selected with the IR observations on these regions (Cushing, Tokunaga & Kobayashi 2000; Wilking, Greene & Meyer 1999). Two out of eight bona fide brown dwarfs (BDs) and five out of ten candidate brown dwarfs (CBDs) are found to be X-ray sources (Imanishi, Tsujimoto & Koyama 2001)³. The X-ray detection rates are, therefore 25% and 50% for BDs and CBDs, respectively. Table 4 shows the list of X-ray detected brown dwarfs together with the best-

Table 4. X-rays from Brown Dwarfs

Name ¹	Sp.type ²	kT^3	N_H^4	L_x^5	$\log(L_x/L_{bol})^6$
Bona fide Brown Dwarf					
GY141	M8	-	-	0.32	-3.5
GY310	M8.5	1.7(0.9-2.2)	0.8(0.5-1.5)	12	-3.2
Candidate Brown Dwarf					
GY31	M5.5	2.2(1.7-2.9)	5.9(5.1-7.2)	120	-3.4
GY37	M6	-	-	0.76	-4.1
GY59	M6	2.5(≥ 1.0)	1.4(0.5-3.0)	3.4	-3.8
GY84	M6	-	-	1.1	-4.5
GY326	M4	0.9(0.7-1.2)	2.3(1.6-3.0)	36	-3.3

Temperatures are fixed to 2.0 keV, for GY141, GY37 and GY84. Parentheses indicate 90% confidence range.

(1), (2), (6) References: Cushing, Tokunaga & Kobayashi (2000); Wilking, Greene & Meyer (1999)

(2) Spectral type, uncertainty is ± 1.5 .

(3) Thin thermal temperature in units of keV

(4) Absorption in units of 10^{22} Hcm⁻²

(5) The 0.5-9 keV band luminosity in units of 10^{28} ergs s⁻¹

(6) Luminosity ratio between X-ray and bolometric

fit parameters of a thin thermal model. The luminosity ratio of X-ray (L_x) to bolometric (L_{bol}), L_x/L_{bol} , lies between $10^{-3} - 10^{-5}$, which is similar to those of low-mass pre-main-sequence stars (e.g., Imanishi, Koyama & Tsuboi 2001) and dMe stars (Giampapa et al. 1996). For the X-ray non-detected BDs and CBDs, the upper limits of L_x/L_{bol} are also scattered around $10^{-3} - 10^{-5}$, comparable with or slightly lower than those of X-ray detected samples. This leads us to suspect that the X-ray non-detected BDs and CBDs may also emit X-rays near at the current sensitivity limit of *Chandra*.

³We call a bona fide brown dwarf (BD) for stars with the stellar mass well below the hydrogen burning limit of $0.08M_\odot$ and a candidate brown dwarf (CBD) for stars in a transition mass region

One BD (GY310) and three CBDs (GY31, GY59 and GY326) are bright enough, hence reliable X-ray spectra and light curves can be made for the first time. The spectra are fitted with a thin thermal plasma model of ~ 2 keV temperature. Solar-like flares are detected from 2 CBDs (GY31 and GY59). These X-ray features are similar to those of low mass stars. Together with the high L_x/L_{bol} value, we suggest that X-rays from these sub-stellar objects (BDs and CBDs) are attributable to magnetic activity similar to low-mass stellar objects.

A debatable issue is the mechanism of magnetic field amplification. Brown dwarfs are fully convective, hence the standard dynamo mechanism may not work. This situation is the same as low mass protostars. One possible scenario is the magnetic arcade scenario connecting a star and disk, which can also be applied for the X-rays from high mass YSOs (see section 3), although stellar structures may be largely different (Tsuboi et al. 2000; Montmerle et al. 2000). If BDs and CBDs emit X-rays with this mechanism, X-ray activity should vanish when the disk disappears as BDs and CBDs evolve, but our observations show no clear evidence for the X-ray evolution with ages. We therefore conclude that an accretion disk is not a key factor for the X-ray emissions from BDs and CBDs. Another type, such as turbulent-driven dynamo (Durney, De Young, & Roxburgh 1993), should be involved.

Acknowledgments. The author expresses his thanks to Drs. Y. Tsuboi, K. Hamaguchi, H. Murakami, K. Imanishi, M. Tsujimoto, M. Kohno and S. Takagi for their collaborations.

References

- André, P. & Montmerle, T. 1994, ApJ, 420, 837
 Aso, Y., Tatematsu, K., Sekimoto, Y., et al. 2000, ApJS, 131, 465
 Beckwith, S., Evans, N. J., Becklin, E. E., Neugebauer, G. 1976, ApJ, 208, 390
 Carkner, L., Kozak, J. A., & Feigelson, E. D. 1998, AJ, 116, 1933
 Carpenter, J.M., Meyer, M.R., Dougados, C., et al. 1997, AJ, 114, 198
 Casanova, S., Montmerle, T., Feigelson, E. D., & André, P. 1995, ApJ, 439, 752
 Chen, H., Myers, P. C., Ladd, E. F., & Wood, D. O. S. 1995, ApJ, 445, 377
 Chen, H., Grenfell, T. G., Myers P. C., & Hughes, J. D. 1997, ApJ, 478, 295
 Cushing, M. C., Tokunaga, A. T., & Kobayashi, N. 2000, AJ, 119, 3019
 De Pree, C. G., Goss, W. M., & Gaume, R. A. 1998, ApJ, 500, 847
 Durney, B. R., De Young, D. S., & Roxburgh, I. W. 1993, Sol. Phys., 145, 207
 Feigelson, E. D. & Montmerle, T. 1999, ARA&A, 37, 363
 Gagne, M., Caillault, J. P., Stauffer, J. R., Linsky, J. 1997, ApJ, 478, L87
 Gaume, R. A., Claussen, M. J., De Pree, C. G., et al. 1995, ApJ, 449, 663
 Giampapa, M. S., Rosner, R., Kashyap, V., et al. 1996, ApJ, 463, 707
 Grosso, N., Montmerle, T., Bontemps, S., et al. 2000, A&A, 359, 113
 Hamaguchi, K., Tsuboi, Y., & Koyama, K. 2000, Adv. Space Res., 25, 531
 Hayashi, M.R., Shibata, K., & Matsumoto, R. 1996, ApJ, 468, L37

- Hofner, P. & Churchwell, E. 1997, ApJ, 486, L39
- Howard, E., Pipher, J. L. & Forrest, W. J. 1994, ApJ, 425, 707
- Imanishi, K., Koyama, K., & Tsuboi, Y. 2001, ApJ, 557, 747
- Imanishi, K., Tsujimoto, M., & Koyama, K. 2001, ApJ, (in press)
- Kamata, Y., Koyama, K., Tsuboi, Y., & Yamauchi, S. 1997, PASJ, 49, 461
- Kohno, M., Koyama, K. & Hamaguchi, K. 2001, ApJ, (submitted)
- Koyama, K., Hamaguchi, K., Ueno, S., et al. 1996, PASJ, 48, L87
- Lis, D. C., Goldsmith, P. F., Carlstrom, J. E., et al. 1993, ApJ, 402, 238
- Luhman, K. L. & Rieke, G. H. 1999, ApJ, 525, 440
- Massi, M., Felli, M., & Simon, M. 1985, A&A, 152, 387
- Mehringner, D. M., Goss, W. M. & Palmer, P. 1994, ApJ, 434, 237
- Montmerle, T., Grosso, N., Tsuboi, Y. & Koyama, K. 2000, ApJ, 532, 1097
- Motte, F., André, P., & Neri, R. 1998, A&A, 336, 150
- Murakami, H., Koyama, K. & Maeda, Y. 2001, ApJ, (in press)
- Neuhäuser, R. & Comerón, F. 1998, Nature, 282, 83
- Racine, R. 1968, AJ, 73, 233
- Reipurth, B. 1999, *A General Catalogue of Herbig-Haro Objects*, 2. Edition
- Reipurth, B., Rodríguez, L. F., & Chini, R. 1999, ApJ, 118, 983
- Schulz, N.S., Canizares, C., Huenemoerder, D., et al. 2001, ApJ, 549, 441
- Sekimoto, Y., Matsuzaki, K., Kamae, T., et al. 2000, PASJ, 52, L31
- Sellgren, K., Brooke, T. Y., Smith, R. G. & Geballe, T. R. 1995, ApJ, 449, L69
- Sellgren, K., Smith, R. G. & Brooke, T. Y. 1994, ApJ, 433, L179
- Smith, R. G., Sellgren, K., & Tokunaga, A. 1989, ApJ, 344, 413
- Takagi, S. Murakami, H., & Koyama, K. 2001, (in preparation)
- Tsuboi, Y., Koyama, K., Hamaguchi, K., et al. 2001, ApJ, 554, 734
- Tsuboi, Y., Imanishi, K., Koyama, K., et al. 2000, ApJ, 532, 1089
- Tsujimoto, M., Koyama, K., Tsuboi, Y., et al. 2001a, ApJS, (submitted)
- Tsujimoto, M., Koyama, K., Tsuboi, Y., et al. 2001b, (in preparation)
- Wilking, B. A., Greene, T. P., & Meyer, M. R. 1999, AJ, 117, 469
- Yamauchi, S., Koyama, K., Sakano, M. & Okada, K. 1997, PASJ, 48, 719
- Yao, Y., Hirata, N., Ishii N., et al. 1997, ApJ, 490, 281
- Yu, K. C., Bally, J., & Devine, D. 1997, ApJ, 485, L45
- Yu, K. C., Billawala, Y., Smith, M. D., et al. 2000, AJ, 120, 1974